AD-A113 525 STANFORD UNIV CA DIV OF APPLIED MECHANICS F/G 20/11
STRESS ANALYSIS FOR KINEMATIC HARDENING IN FINITE-DEFORMATION P--ETC(U)
DEC 81 E H LEE, R L MALLETT, T B WERTHEIMER N00014-81-K-0660
UNCLASSIFIED SUDAM-81-11 NL

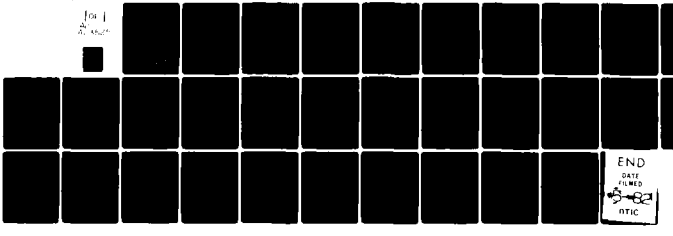

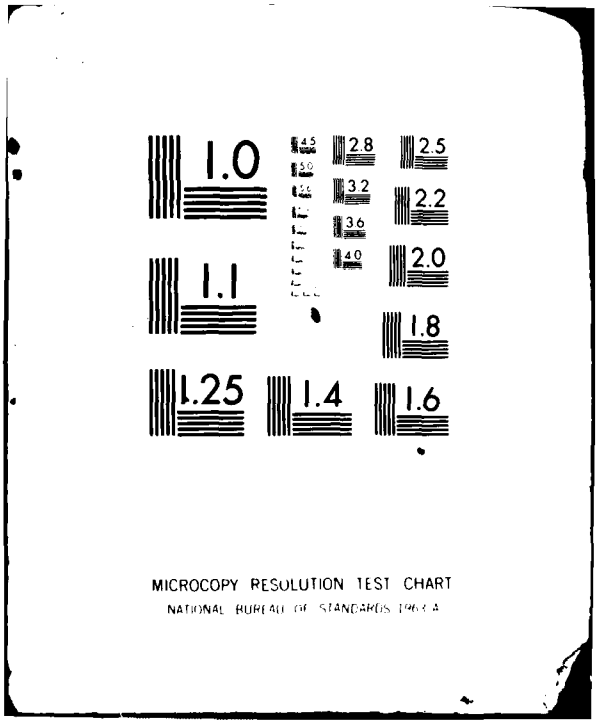
1.0
1.1
1.25
1.4
1.6
1.8
2.0
2.2
2.5
2.8
3.2
3.6
4.0
4.5
5.0
MICROCOPY RESOLUTION TEST CHART
NATIONAL BUREAU OF STANDARDS 1963-A

Office of Naval Research
Department of the Navy
Scientific Report
Contract N00014-81-K-0660

STRESS ANALYSIS FOR KINEMATIC HARDENING IN FINITE-DEFORMATION PLASTICITY

By

E. H. Lee, R. L. Mallett and

T. B. Wertheimer

SUDAM Report No. 81-11

December 1981

DIVISION
OF
APPLIED
MECHANICS

DEPARTMENT
OF
MECHANICAL
ENGINEERING

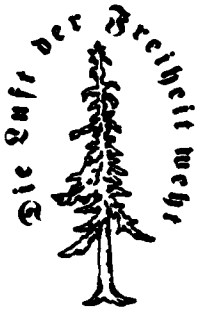

STANFORD
UNIVERSITY
STANFORD,
CALIFORNIA
94305

Stress Analysis for Kinematic Hardening in Finite-Deformation Plasticity

E. H. Lee and R. L. Mallett, Rensselaer Polytechnic Institute and Stanford University, and

T. B. Wertheimer, MARC Analysis Research Corp. and Stanford University

Abstract

Kinematic hardening represents the anisotropic component of strain hardening by a shift, $\underset{\sim}{\alpha}$, of the center of the yield surface in stress space. The currently adopted approach in stress analysis at finite deformation (in which time derivatives of $\underset{\sim}{\alpha}$ and of stress appear respectively in the evolution equation for $\underset{\sim}{\alpha}$ and in the flow type constitutive equation) accounts for the effect of rotation by using Jaumann derivatives based on the spin (the skew-symmetric part of the velocity gradient). This guarantees objectivity under superimposed time-dependent rigid-body rotations. However the analysis generates the unexpected result that oscillatory shear stress is predicted for monotonically increasing simple shear strain.

The simple shear strain growing at constant rate $\dot{\gamma} = k$ yields a spin in the plane of shearing having the constant magnitude $k/2$. The effect of this on the evolution equation for the shift tensor $\underset{\sim}{\alpha}$ causes the latter to rotate continuously. In contrast, the kinematics of simple shear prescribe that no material directions rotate by more than π radians. Together these two features seem inconsistant since the shift tensor or back stress has its origin embedded in the material, for example as rows of dislocations piled up against grain boundaries or inclusions.

By defining a modified Jaumann derivative based on the angular velocity of certain directions embedded in the body which characterize the effective resultant orientation of the micro-mechanisms responsible for the anisotropic hardening, a method of stress analysis is implemented which eliminates the inconsistency and yields a monotonically increasing shear stress. Features which support the validity of this approach are presented.

1. Introduction

In an intriguing paper [1]*, Nagtegaal and de Jong evaluated the stresses generated by simple shear to large deformation in elastic-plastic and rigid-plastic materials which exhibit anisotropic hardening. In conformity with current practice for finite deformation in the case of kinematic hardening, they used an evolution equation for the back stress or shift tensor $\underset{\sim}{\alpha}$ (the current center of the yield surface) which relates the Jaumann derivative of $\underset{\sim}{\alpha}$ to the plastic strain rate. This incorporates effects of finite rotation and ensures objectivity of the evolution equation under rigid-body rotations. They obtained the unexpected result, for a material which strain hardens monotonically in tension, that the shear traction grows to a maximum value at a shear strain γ of the order unity and then oscillates with increasing strain with a period of about six. Similar behavior was exhibited by the normal traction on the shearing planes which was initially compressive. Of course such a variation would not occur in practice because of the onset of instability, but large shear strains have occurred in experiments without instability. Other anisotropic hardening models, such as that due to Mroz, did not generate oscillations in the shear traction.

A study of the analytical structure of the kinematic hardening law shows that, in the case of simple shear, the use of the conventional Jaumann derivative based on the spin causes the shift tensor $\underset{\sim}{\alpha}$ to rotate continuously and this generates oscillations in the stress field. In the present paper it is also shown that this analytical structure, which is currently adopted

---

* Numbers in brackets denote references collected at the end of the paper.

in finite-deformation elastic-plastic codes involving kinematic hardening, is not in accord with the effects of the physical micromechanisms which produce plastic flow. A modified theory consonant with these yields a monotonically increasing shear traction for the problem under discussion.

2. The Kinematics of Simple Shear

Using rectangular Cartesian coordinates for the configuration at the time t, we consider simple shear in the x_1-direction, as depicted in Fig.1, defined by the displacements

$$u_1 = k t x_2 , \quad u_2 = u_3 = 0 . \tag{2.1}$$

This corresponds to the steady-state velocity field

$$v_1 = k x_2 , \quad v_2 = v_3 = 0 \tag{2.2}$$

and the velocity gradient tensor

$$\underset{\sim}{L} = \frac{\partial v_i}{\partial x_j} = \begin{bmatrix} 0 & k & 0 \\ 0 & 0 & 0 \\ 0 & 0 & 0 \end{bmatrix} \tag{2.3}$$

with the rate of deformation $\underset{\sim}{D}$ and the spin $\underset{\sim}{W}$ given by the symmetric and skew-symmetric parts, respectively:

$$\underset{\sim}{D} = \begin{bmatrix} 0 & k/2 & 0 \\ k/2 & 0 & 0 \\ 0 & 0 & 0 \end{bmatrix} ; \quad \underset{\sim}{W} = \begin{bmatrix} 0 & k/2 & 0 \\ -k/2 & 0 & 0 \\ 0 & 0 & 0 \end{bmatrix} \tag{2.4}$$

The velocity field is thus steady with constant rate of shear strain $\dot{\gamma} = k$ and constant spin $\underset{\sim}{W}$ with angular speed k/2.

Figure 2 illustrates the superposition of the deformation rate and spin components of the velocity field, the arrows expressing the

angular velocities of lines of material points currently parallel to the x_1 and x_2 axes, respectively. It is seen that those parallel to the x_2-axis rotate with angular velocity k while those parallel to the x_1-axis do not rotate.

Figure 1 shows the deformation at times t_1 and t of an initially unit square block, with sides initially on the x_1 and x_2 axes. Because of the linear velocity field, straight lines defined by material points remain straight and the square block is deformed into a sequence of parallelograms. The line of material particles OA_o, initially on the x_2-axis, deforms to OA_1 and OA at times t_1 and t, respectively. Clearly it will only approach the x_1-axis as time approaches infinity, so that the maximum angular rotation for this line of material points is $\pi/2$.

Because the velocity field is steady and the velocity gradient is uniform or homogeneous over the body, the angular velocity of a line of particles in the (x_1,x_2) plane of shear depends only on its orientation. Thus, the description in the previous paragraph of the motion of the side OA_o of the unit square can be applied to every line of material points. Thus the inclination of a line of material points to the x_1-axis [$\theta(t)$ in Fig.1 for OA] can be used to express the angular velocity $\dot{\theta}$ of the line.

From Fig.1 the length of OA is $1/\sin\theta$, the point O is at rest and the component of the velocity of A normal to OA is $k \sin\theta$ in the direction of θ decreasing. Hence its angular velocity $\dot{\theta}$ is given by

$$\dot{\theta} = -k \sin^2\theta \qquad (2.5)$$

which, as explained in the previous paragraph, is applicable to all lines of material points in the x_1, x_2 plane. Integration of (2.5), or observing in Fig.1 that the projection of OA onto the x_1 axis is $\cot\theta$ and that A moves

with velocity k along the line $x_2 = 1$, gives the following expression for the varying inclination θ of a line of material points corresponding to θ_o at time t_o:

$$\cot \theta = \cot \theta_o + k(t - t_o) . \tag{2.6}$$

This again applies to all lines with inclination θ_o at time t_o irrespective of their position.

Thus the total possible rotation of lines of material particles is limited since, unless they are parallel to the x_1 axis, in which case they do not rotate, all lines rotate with negative $\dot{\theta}$ towards the x_1 axis ($\theta = 0$). The largest rotation is of lines which initially have the inclination $\theta = \pi - \epsilon$, ϵ small and positive. They initially have a small negative $\dot{\theta}$ which increases in magnitude to k as they become parallel to the x_2 axis and then falls in magnitude monotonically towards zero as the lines approach the x_1 axis. The total angle of rotation approaches $\pi - \epsilon$.

Note that the angular velocity of the lines $\theta = \pm\pi/4$, which coincide with the principal directions of the deformation rate tensor $\underset{\sim}{D}$, is k/2, equal to the spin as it should be. This is also the average of the angular velocities over all directions in the current configuration.

3. The Currently Adopted Analysis for Finite Deformation

The back-stress $\underset{\sim}{\alpha}$ which prescribes the position of the center of the yield surface in stress space provides the anisotropy in the yield function needed to incorporate such effects as the Bauschinger effect. Since the source of this property is embedded in the material, the tensor $\underset{\sim}{\alpha}$ is considered to rotate with the material so that the conventional Jaumann derivative (rate of change of $\underset{\sim}{\alpha}$ components based on axes spinning with the material) has commonly been used in the evolution equation for $\underset{\sim}{\alpha}$. Thus changes in $\underset{\sim}{\alpha}$

due to material spin are eliminated leaving only changes associated with the history of plastic strain. This ensures spin-invariance or objectivity under superimposed rigid-body rotation. A commonly used evolution relation for $\underset{\sim}{\alpha}$ is that given by Mróz, Shrivastava and Dubey [2] for combined isotropic-kinematic hardening, modified for finite-deformation applications, as already mentioned, by introducing the Jaumann derivative

$$\overset{\circ}{\underset{\sim}{\alpha}} = C_1(\bar{\varepsilon}^p)(\underset{\sim}{s} - \underset{\sim}{\alpha}) \tag{3.1}$$

where $\underset{\sim}{s}$ is the stress deviator,

$$\bar{\varepsilon}^p = \int_0^t \sqrt{2D^p_{ij} D^p_{ij}/3}\, dt \tag{3.2}$$

is the generalized plastic strain invariant and the superscript o signifies the Jaumann derivative. Because of normality for the plastic strain rate

$$\underset{\sim}{D}^p \sim (\underset{\sim}{s} - \underset{\sim}{\alpha}) \tag{3.3}$$

and thus (3.1) can be expressed in the form

$$\overset{\circ}{\underset{\sim}{\alpha}} = C_2(\bar{\varepsilon}^p, \text{ strain history})\underset{\sim}{D}^p \tag{3.4}$$

This is more convenient for the discussion in this paper since the deformation is prescribed. Moreover the aspect of the analysis which we wish to discuss can be adequately studied on the basis of rigid-plastic theory since the elastic strains are negligible compared with the large plastic strains. Hence we can replace $\underset{\sim}{D}^p$ in (3.4) by $\underset{\sim}{D}$. For simplicity of explanation, we shall limit our consideration to kinematic hardening although the approach applies equally well to combined kinematic-isotropic hardening.

In order to examine how $\underset{\sim}{\alpha}$ changes with respect to the axes (x_1, x_2) fixed in space, we need the material derivative of the shift tensor, $\dot{\underset{\sim}{\alpha}}$, and this is deducible from the expression for the Jaumann derivative

$$\overset{\circ}{\underset{\sim}{\alpha}} = \dot{\underset{\sim}{\alpha}} - \underset{\sim}{W}\underset{\sim}{\alpha} + \underset{\sim}{\alpha}\underset{\sim}{W} \tag{3.5}$$

Using (3.4) this gives

$$\dot{\underset{\sim}{\alpha}} = C_2 \underset{\sim}{D}^p + \underset{\sim}{W}\underset{\sim}{\alpha} - \underset{\sim}{\alpha}\underset{\sim}{W} \tag{3.6}$$

The last two terms express the contribution to the change in $\underset{\sim}{\alpha}$ due to the spin $\underset{\sim}{W}$, which in the case of simple shear has the constant value given in (2.4). The corresponding angular velocity in the (x_1,x_2) plane is $k/2$, so that the angle turned through by $\underset{\sim}{\alpha}$ due to $\underset{\sim}{W}$ in a time increment Δt is $k\Delta t/2$, and this must be combined with the contribution of the first term on the right-hand side of (3.6). For rigid-plastic theory of simple shear the latter term adds increments to $\underset{\sim}{\alpha}$ which have the same principal directions as the deformation rate $\underset{\sim}{D}$, corresponding to $\theta = \pi/4$ and $3\pi/4$.

The continuing rotation of $\underset{\sim}{\alpha}$ in the (x_1,x_2) plane is in marked contrast with the rotation of lines of material points in the body for which the total rotation varies with the initial orientation but can never exceed π. Since the hardening mechanisms are embedded in the material it seems, on physical grounds, implausible that the macroscopic hardening parameter $\underset{\sim}{\alpha}$ could continue to rotate through an unlimited angle while no elements of the material do. Moreover the oscillations in stress obtained by using the current theory appear to be associated with the continuing rotation of $\underset{\sim}{\alpha}$. The period of the stress oscillations with respect to the shear strain $\gamma = kt$ is approximately equal to 2π. With this strain increment, the rotation $(k/2)t$ will change by π. But a tensor rotated by π about a principal eigenvector, x_3 in the present case, will be unchanged. Thus this simple assessment is in conformity with the calculated stress variation. The assessment is approximate since it does not take into account the strain rate term in (3.6).

The spin $\underset{\sim}{W}$ is the average of the angular velocities exhibited by all material lines passing through a point. Spin would thus seem to be an appropriate variable to include in a formulation for isotropic hardening for which no specific directions have special influence. But kinematic hardening is an anisotropic phenomenon for which specific material directions play a significant role. Moreover the micromechanisms which generate anisotropic hardening, such as pile-up of dislocations against grain boundaries or inclusions, are associated with specific directions embedded in the material and the rotation of these particular directions or an average over such active directions should play a special role in formulating the macroscopic constitutive relation. A law based on this concept is suggested in the following section.

4. A Modified Constitutive Relation

In view of the discussion in the previous section, it is necessary to determine a direction embedded in the material which characterizes the anisotropy induced by previous plastic flow. As a simple example which may be appropriate for simple shear, we select the direction associated with the maximum eigenvalue of the shift tensor $\underset{\sim}{\alpha}$. Justification for this choice is discussed later in this section. In expressing the influence of current plastic flow on the evolution of $\underset{\sim}{\alpha}$ we must eliminate the change in $\underset{\sim}{\alpha}$ caused by the rotation of micromechanisms responsible for the current hardening. Thus we define a modified Jaumann type derivative which eliminates the effect of rotation of the material elements lined up in the direction of the eigenvector of $\underset{\sim}{\alpha}$ associated with the maximum eigenvalue. This rotation defines a spin $\underset{\sim}{W}^*$ corresponding to the angular velocity given by (2.5) with the appropriate value of θ. We retain the influence of current plastic flow

due to Mróz et al. [2] and obtain the evolution equation analogous to (3.4)

$$\overset{*}{\underset{\sim}{\alpha}} = C_2 \underset{\sim}{D}^p \tag{4.1}$$

where the superscript * denotes the modified Jaumann derivative associated with the spin $\underset{\sim}{W}^*$

$$\overset{*}{\underset{\sim}{\alpha}} = \dot{\underset{\sim}{\alpha}} - \underset{\sim}{W}^* \underset{\sim}{\alpha} + \underset{\sim}{\alpha} \underset{\sim}{W}^* \tag{4.2}$$

Thus $\dot{\underset{\sim}{\alpha}}$, the material time derivative of $\underset{\sim}{\alpha}$ with respect to fixed axes (x_1, x_2), is given by

$$\dot{\underset{\sim}{\alpha}} = C_2 \underset{\sim}{D}^p + \underset{\sim}{W}^* \underset{\sim}{\alpha} - \underset{\sim}{\alpha} \underset{\sim}{W}^* \tag{4.3}$$

When shearing commences the eigenvector of $\underset{\sim}{\alpha}$ under consideration first grows in the direction $\theta = \pi/4$ but the motion of the material continually tends to reduce this angle due to the rotation effect of the last two terms in (4.3). As the angle θ decreases the spin term $\underset{\sim}{W}^*$ decreases according to (2.5) but θ will remain positive. It is to be expected that such behavior will eliminate the oscillations in the shear traction obtained by using the evolution equation (3.6) based on the conventional Jaumann derivative.

Note that the new evolution equation (4.1) is objective under rigid-body rotation since the spin $\underset{\sim}{W}^*$ is determined from the tensor $\underset{\sim}{\alpha}$ without reference to the axes adopted and is additive with respect to superposed rigid body spin.*

In selecting the effective direction of action of the anisotropic hardening mechanisms which are embedded in the material, one must bear in mind that we are concerned with polycrystalline materials so that no specific global slip planes exist as are determined by the lattice structure in the case of single crystals. The direction must thus be an effective average over the response of the individual crystallites. Thus simple shear is not likely to occur only by slip over planes adjacent to the x_1-axis as depicted

*see the Appendix.

in Fig.1, since the complementary shear stress will be acting parallel to the x_2-axis, and this will cause shear strain in some crystallites, which, combined with rotation, will contribute to global simple shear. Thus in selecting the evolution law (4.1) we envisaged shears associated with both planes yielding an effective anisotropic contribution. This is in conformity with the evolution equation due to Mróz et al. [2]. These contributions were then summed, allowing for rotation of the earlier contributions, by integrating (4.3) to yield $\underset{\sim}{\alpha}$ which determines the resultant anisotropic hardening.

Because of the lack of influence of hydrostatic pressure on plastic flow, the yield condition is a stress deviator relation and thus $\underset{\sim}{\alpha}$ is a stress deviator so that, in the case of simple shear with no deformation in the x_3-direction, the D_{33} component is zero and hence the two nonzero eigenvalues of $\underset{\sim}{\alpha}$ have the same absolute magnitude. We chose the tensile strain-rate orientation to express the effective anisotropic hardening mechanism direction. The associated line-up of material elements in the tensile direction rotate more slowly (initial angular velocity k/2 and decreasing) than in the compressive strain-rate direction (initial angular velocity k/2 and increasing) and hence the former will yield a greater corresponding eigenvalue of the resulting tensor $\underset{\sim}{\alpha}$ and so comprise the dominant back-stress direction. The elements lined up in the compression direction will rotate towards the orientation which has the angular velocity k, and adding increments with more rapidly varying orientation will inhibit the increase in the associated eigenvalue.

We suggest that the recipe for the spin $\underset{\sim}{W}^*$ can be extended to general three-dimensional deformation by taking $\underset{\sim}{W}^*$ to be determined by the eigenvector associated with the maximum absolute value of the eigenvalues of $\underset{\sim}{\alpha}$. The spin is determined by the rotation of the line of material elements instantaneously

coinciding with that eigenvector. Rotation around this direction could be determined by the motion of material points on the eigenvector corresponding to the next largest eigenvalue. This selection of specific eigenvectors could lead to nonsmooth response analogous to the Tresca yield condition, but this could perhaps be avoided by taking an average over possible hardening mechanisms which would result in a smoother response.

This approach to anisotropic hardening exhibits the property, necessary for application, that measurement of the yield surface (assumed to be consistent with combined isotropic-kinematic hardening) supplies the information needed to formulate the constitutive relation for the analysis of subsequent deformation. The shift tensor $\underset{\sim}{\alpha}$ and the square of the radius of the yield surface given by the trace of the tensor product

$$(\underset{\sim}{s} - \underset{\sim}{\alpha}) : (\underset{\sim}{s} - \underset{\sim}{\alpha}) = \frac{2}{3}\sigma_o^2 \tag{4.4}$$

comprise all that is needed concerning the previous history of plastic deformation.

5. Stress Analysis

The theory for combined isotropic-kinematic hardening for infinitesimal deformation presented by Mróz et al. [2] is adapted for finite deformation applications by using the appropriate Jaumann type derivative of stress just as the modified Jaumann derivative was developed for use in the evolution equation for the back-stress $\underset{\sim}{\alpha}$.

Since we are investigating a large deformation problem, rigid-plastic theory is applied in order to obtain a relatively simple analysis although an elastic-plastic solution is also presented for comparison with the rigid-plastic case. Since we are considering a problem involving homogeneous

deformation, plastic flow is occurring throughout the body, and in this case stress analysis on the basis of rigid-plastic theory is not restricted by the existence of extensive rigid regions as commonly arises in metal-forming problems [3]. The velocity boundary conditions for simple shear (Fig.1) prescribe an incompressible motion and since the rigid-plastic constitutive relation is incompressible, the stress can only be determined to within an arbitrary hydrostatic pressure. Thus stress deviators are evaluated.

The yield condition for combined kinematic-isotropic hardening is given by (4.4) with

$$\sigma_o = \sigma_o(\bar{\varepsilon}^p) \tag{5.1}$$

where $\bar{\varepsilon}^p$ is the generalized plastic strain invariant (3.2) and $\underset{\sim}{\alpha}$ is the back-stress given by the evolution equation (4.1).

The tensor $\underset{\sim}{\alpha}$ and hence the yield surface will in general be rotating so that care must be exercised in expressing the stress rate to be used in the equation for the strain rate associated with strain hardening. The rotation of $\underset{\sim}{\alpha}$ is determined by integration of the evolution equation (4.3). The corresponding spin, $\underset{\sim}{W}^{\alpha}$, of the orthogonal eigen-vector triad differs from $\underset{\sim}{W}^*$ because of the $\underset{\sim}{D}^p$ term in (4.3). The Jaumann stress rate associated with the angular velocity $\underset{\sim}{W}^{\alpha}$ gives the rate of increase of stress when the change due to this spin has been subtracted off. If this Jaumann stress rate were zero, then due to spin there would be no change in stress relative to the yield surface. Thus this modified Jaumann derivative of the stress is the quantity which expresses the strain-hardening rate. Thus utilizing the normality requirement for the plastic strain rate (3.3) and the component of the stress rate in that direction

$$[(\underset{\sim}{s}-\underset{\sim}{\alpha})/|\underset{\sim}{s}-\underset{\sim}{\alpha}|]:\overset{\alpha}{\underset{\sim}{s}} = \left[(\underset{\sim}{s}-\underset{\sim}{\alpha})/\sqrt{\tfrac{2}{3}}\,\sigma_o\right]:\overset{\alpha}{\underset{\sim}{s}} \tag{5.2}$$

using (4.4) and writing $\overset{\alpha}{\underset{\sim}{s}}$ for the new modified Jaumann rate associated with spin $\underset{\sim}{W}^{\alpha}$, the plastic strain rate is given by

$$\underset{\sim}{D}(=\underset{\sim}{D}^{p}) = \frac{3}{2h\sigma_o^2}(\underset{\sim}{s}-\underset{\sim}{\alpha})[(\underset{\sim}{s}-\underset{\sim}{\alpha}):\overset{\alpha}{\underset{\sim}{s}}] \quad . \tag{5.3}$$

where h is a strain hardening modulus. This is Eq. (11) of [2] suitably modified for finite deformation. Note that the trace of the tensor product is expressed by

$$(\underset{\sim}{s}-\underset{\sim}{\alpha}):\overset{\alpha}{\underset{\sim}{s}} = (s_{ij}-\alpha_{ij})\overset{\alpha}{s}_{ji} = (\underset{\sim}{s}-\underset{\sim}{\alpha})\cdot\overset{\alpha}{\underset{\sim}{s}} \tag{5.4}$$

where the last form is the scalar product of the tensors expressed as vectors in nine-dimensional stress space. Note that the operator L in (5.3) ($D^{p}_{ij} = L_{ijkl}\overset{\alpha}{s}_{kl}$) embodies the symmetries in (i,j), (k,l) and (ij,kl).

In the usual finite-element computer-code procedure for elastic-plastic analysis, the equivalent of (5.3) with $\underset{\sim}{D}$ containing elastic terms in stress rate, would be solved for $\overset{\alpha}{\underset{\sim}{s}}$ and the evolution equation (4.1) for $\overset{*}{\alpha}$. Thus $\underset{\sim}{s}$ and $\underset{\sim}{\alpha}$ can be updated to proceed with the next step. However, in the present case $\overset{\alpha}{\underset{\sim}{s}}$ only appears in the scalar quantity in square brackets in (5.3), so that these equations are severely underdetermined for evaluating $\overset{\alpha}{\underset{\sim}{s}}$. But since $(\underset{\sim}{s}-\underset{\sim}{\alpha})$ satisfies (4.4) with (5.1) and (3.2), $\underset{\sim}{D}=\underset{\sim}{D}^{p}$ with (3.3) [also implied by (5.3)] permits $(\underset{\sim}{s}-\underset{\sim}{\alpha})$ to be updated and combining this with the evolution equation (4.1) for $\overset{*}{\underset{\sim}{\alpha}}$ permits $\underset{\sim}{s}$ and $\underset{\sim}{\alpha}$ to be updated. This procedure was carried out for the simple shear problem.

An elastic-plastic solution was also computed with the MARC program by modifying the spin term in the Jaumann derivative from $\underset{\sim}{W}$ to $\underset{\sim}{W}^{*}$, and replacing the Jaumann derivative $\overset{\alpha}{\underset{\sim}{s}}$ by $\overset{*}{\underset{\sim}{s}}$ since the spin of material elements instantaneously coincident with the eigen-vectors of $\underset{\sim}{\alpha}$ is likely to be close to the spin of the eigenvectors themselves.

6. Comparison of Solutions

A solution was evaluated using the rigid-plastic model with the initial tensile yield stress Y = 207 MPa(30 ksi) and linear tensile work hardening with modulus

310 MPa(45 ksi). These values are appropriate to model an aluminum alloy. The constant strain-hardening modulus in tension implies that C_2 is a constant in (4.1).

Figure 3 shows the variation of the component of the spin associated with the material motion related to the back-stress tensor $\underset{\sim}{\alpha}$. For the currently accepted approach this remains constant at (-k/2). When the rotation of a locus of material particles which carry the back-stress determines the evolution of $\underset{\sim}{\alpha}$ as suggested in this paper, the magnitude of the spin commences at k/2 and decreases rapidly. Strain steps of $\Delta\gamma = 0.1$ were used in the calculation in view of the range of strain up to $\gamma = 10$ and, without iteration, two steps were completed before deviation from the initial value (-k/2) was predicted. In view of the stress results it did not seem necessary to refine the strain increment size to improve the spin $\underset{\sim}{W}^*$. Figure 4 shows the inclination to the x_1-axis of the controlling eigenvector of $\underset{\sim}{\alpha}$. On reaching -90°, the plotting routine jumps automatically to +90°. The continuing rotation associated with spin $\underset{\sim}{W}$ is in clear contrast to the limited rotation towards the x_1-axis with $\underset{\sim}{W}^*$,

Figure 5 shows the deduced shear stress versus shear strain curves. The use of the conventional Jaumann derivative gives the oscillations presented in [1]. The modified theory is seen to yield a curve which agrees closely with the currently utilized approach up to a shear strain γ of unity, but thereafter the stress increases monotonically with a continuously decreasing modulus. The straight line relation shown is deduced from the tensile behavior on the basis of isotropic hardening with Mises yield condition.

Figure 6 shows the variation of the stress-deviator component in the direction of the x_1-axis. Appreciable deviation of the two solutions occurs earlier than for shear stress, at a strain of about 0.5. Otherwise the contrast between the two solutions is similar to the shear results. However, isotropic hardening predicts no normal stress deviators s_{11} and s_{22}.

Figures 7 and 8 show the stress-shear strain variations deduced using the MARC elastic-plastic code suitably modified, as already mentioned, assuming a Young's modulus of 6.90×10^4 mPa (10×10^6 psi) and a Poisson's ratio of 0.3. Because of the strain steps of magnitude 0.1, the initial elastic response is not accurately predicted and for the longitudinal deviator component an initial slight instability occurs which quickly dies down. Because the elastic-plastic constitutive equation permits dilatation, stresses (not simply stress deviators) can be predicted. Since plastic flow is considered to be incompressible, and the velocity boundary conditions are consistent with the total deformation being incompressible, and moreover since the plastic flow is homogeneous, the elastic dilatation should be zero and hence also the average hydrostatic tension. The direct stresses in the shearing plane σ_{11} and σ_{22} were found to be almost equal in magnitude to within 0.1% but opposite in sign which is consistent with a zero hydrostatic stress value and zero σ_{33}.

All solutions are presented on the same plots in Figs. 9 and 10. Closer agreement between the rigid-plastic and elastic-plastic solutions is obtained with the new theory. This is to be expected since the much smoother behavior will yield greater numerical accuracy and a discrepancy due to the inclusion of elasticity is likely to be negligible at such large strains. Thus the results are compatible with the loss of numerical accuracy associated with strain steps of magnitude $\Delta\gamma = 0.1$, with perhaps some minor effect of replacing $\overset{\alpha}{\underset{\sim}{s}}$ by $\overset{*}{\underset{\sim}{s}}$ in the elastic plastic calculation. The close agreement of the elastic-plastic finite-element solution may seem surprising in view of the severe element distortion at shear strains $\gamma = 10$. However , it must be borne in mind that the velocity variation is linear which can be modeled exactly by the finite elements even when distorted.

7. Discussion

In addition to the two kinematic hardening stress-strain curves depicted in Fig.5, a linear relation is also shown corresponding to isotropic hardening

according to the Mises yield condition and the linear work-hardening tensile relation. The latter is also the basis for the other curves. Kinematic hardening, according to the theory presented in this paper, initially gives the same shear stress and hardening modulus but the latter decreases monotonically with increasing strain so that at large strains the kinematic hardening curve is well below the isotropic hardening curve. The reason for the falling off of the tangent modulus at large strains in shear is that, due to the material rotation, the principal back-stress direction approaches the x_1-axis, which would correspond to maximum stress for tensile strain in that direction. The shear-stress component in that direction is therefore not so enhanced. This predicted softening tendency in shear compared with isotropic hardening could have significant implications in instability and localization phenomena. As already mentioned, isotropic hardening produces no normal stress s_{11} and s_{22}.

Although oscillations have been observed in the shear stress in torsion experiments, they appear to be unrelated to the oscillations predicted by the application of the conventional Jaumann derivative in the kinematic-hardening analysis. Robbins, Wagenaar, Shepard and Sherby [4] encountered oscillations when loading at high strain rates. Although the strain scale was omitted from Fig.12 of that paper, Professor Sherby assures us that the period was much less than 6. Moreover the measurements made at two values of strain rate indicate that the oscillation was associated with mechanical vibration caused by rapid loading. At lower strain rate the period in terms of strain was reduced, roughly in proportion to the strain rate, indicating a fixed period in time rather than strain. Aernoudt and Sevillano [5] observed instability in the torque which they ascribed to adiabatic heating.

Comparison of the analyses with the conventional and the modified Jaumann derivatives indicates that up to strains near 0.5 the difference in the solutions is small. For strains near 2 the difference reaches about 40% and grows rapidly with increasing strain.

When deformation commences in a virgin isotropic material, the shift tensor is $\underset{\sim}{0}$ and according to (4.1) grows initially in proportion to the deformation rate $\underset{\sim}{D}$, hence its principal directions coincide with those of $\underset{\sim}{D}$. Since the shear-rate components in these directions are zero, these directions rotate according to the spin tensor $\underset{\sim}{W}$ which is thus equal to the spin rate of these material elements $\underset{\sim}{W}^*$. Thus initially the evolution equations (3.4) and (4.1) coincide and will approximate each other until the deformations become appreciable. Thus, as was pointed out in the previous paragraph in connection with the results shown in Figs.5 and 6 for the simple shear case, the formulation in current use can approximate the approach suggested in this paper for moderate finite strains. One might therefore delineate two categories of finite strain termed moderate finite strain and large finite strain. The approach in current use would be adequate in most cases of generalized plastic strain below, say, 0.5 with the new analysis in general needed for larger strains.

It seems to us that the difficulty considered in this paper arises because of an over-simplified interpretation of the significance of the term "spin." A glance at Fig.2 indicates the marked effect of deformation on the angular velocity of lines of material elements in a body. In the case of simple shear this leads to the, on the face of it, surprising result that a constant spin for all time leaves a material line which does not rotate. In the case of anisotropic hardening this variation in rotation of material elements can have a major influence on macroscopic stress distributions.

We have suggested a generally applicable formulation of anisotropic hardening theory, but have only considered a simple example and have chosen a simple hypothesis for the macroscopic influence of the micromechanisms which generate anisotropic hardening. Clearly a thorough study of this

aspect of the theory is called for. This requires an analysis of the micromechanics of polycrystalline material which may involve continuum mechanics type investigations of the interaction between the crystallites. As an example, the backstress may be considered as due to pile-up of dislocations at crystallite boundaries or alternatively as residual stresses generated in the structure of anisotropic crystallite components. With large deformation the changes in crystallite stress and configuration, or alternatively speaking, of the orientation of micromechanisms, can greatly influence the plastic anisotropy. Such investigations to assess the validity of the macroscopic law suggested in this paper are needed, since anisotropic hardening theory incorporates more intricate details of the physical phenomenon than does the simpler isotropic theory.

While the hardening modulus selected is appropriate for an aluminum alloy at moderate strains, hardening would tend to saturate at the large strains considered and so the effect of hardening is no doubt exaggerated in the evaluations presented. Moreover, since kinematic hardening only was assumed, rather than combined kinematic-isotropic hardening, the anisotropic effects are emphasized. These characteristics were not only selected for simplicity of presentation and evaluation, but also to contrast clearly the influence of anisotropic hardening.

As a final comment, the study of localization of plastic flow and the consequent generation of shear bands involves large shear strains so that analysis of the type discussed in this paper will be needed for materials exhibiting anisotropic hardening. Moreover, as mentioned earlier, even with linear strain hardening in tension, the convex upward stress-strain relationship in shear, evident in Fig.5, will increase the tendency for instabilities to be generated.

Acknowledgement

We wish to thank Dr. J.C. Nagtegaal of MARC Analysis Research Corporation for helpful discussion while this work was being formulated.

REFERENCES

1. J.C. Nagtegaal and J.E. de Jong, "Some Aspects of Nonisotropic Work-hardening in Finite Deformation Plasticity," to appear in Proceedings of the Workshop: Plasticity at Finite Deformation, Division of Applied Mechanics, Stanford University, Stanford, California, 1981.

2. Z. Mróz, H.P. Shrivastava and R.N. Dubey, "A Nonlinear Hardening Model and its Application to Cyclic Loading," Acta Mechanica, 25, 51-56, 1976.

3. E.H. Lee, R.L. Mallett and R.M. McMeeking, "Stress and Deformation Analysis of Metal-Forming Processes," Numerical Modelling of Manufacturing Processes, ASME Symposium PVP-PB-025, eds. R.F. Jones, Jr., H. Armen and J.T. Fong, 1977.

4. J.L. Robbins, H. Wagenaar, O.C. Shepard and O.D. Sherby, "Torsion Testing as a Means of Assessing Ductility at High Temperatures," J. of Materials, 2, 2, 271-299, ASTM, 1977.

5. E. Aernoudt and J.G. Sevillano, "Influence of the Mode of Deformation on the Hardening of Ferritic and Pearlitic Carbon Steels at Large Strains," J. of Iron and Steel Inst., 718-725, October 1973.

Appendix: Objectivity

Since Jaumann type derivatives based on several spins are considered in this development, it is perhaps worthwhile to write down explicitly the justification for the objectivity of the analysis. This involves investigating the superposition on a solution of a time-dependent rigid-body rotation expressed by the proper orthogonal matrix $\underset{\sim}{Q}(t)$.

For the deformation gradient $\underset{\sim}{F} = \partial x_i / \partial X_j$, where x_i are the deformed coordinates and X_i the undeformed reference ones, rotation $\underset{\sim}{Q}(t)$ of the deformed configuration gives the transformation

$$\underset{\sim}{F} \rightarrow \underset{\sim}{Q}\,\underset{\sim}{F} \tag{a.1}$$

Thus the derivative of $\underset{\sim}{F}$ at fixed undeformed coordinate (therefore a material or convected derivative) obeys the transformation

$$\dot{\underset{\sim}{F}} \rightarrow \dot{\underset{\sim}{Q}}\,\underset{\sim}{F} + \underset{\sim}{Q}\,\dot{\underset{\sim}{F}} \tag{a.2}$$

Thus $\dot{\underset{\sim}{F}}\,\underset{\sim}{F}^{-1}$, the velocity gradient in the deformed configuration gives

$$\dot{\underset{\sim}{F}}\,\underset{\sim}{F}^{-1} \rightarrow \dot{\underset{\sim}{Q}}\,\underset{\sim}{Q}^{T} + \underset{\sim}{Q}\,\dot{\underset{\sim}{F}}\,\underset{\sim}{F}^{-1}\,\underset{\sim}{Q}^{T} \tag{a.3}$$

Writing the symmetric part, the rate of deformation, $\underset{\sim}{D} = (\dot{\underset{\sim}{F}}\,\underset{\sim}{F}^{-1})_S$ and the anti-symmetric part, the spin, $\underset{\sim}{W} = (\dot{\underset{\sim}{F}}\,\underset{\sim}{F}^{-1})_A$ yields

$$\underset{\sim}{D} \rightarrow \underset{\sim}{Q}\,\underset{\sim}{D}\,\underset{\sim}{Q}^{T} \tag{a.4}$$

$$\underset{\sim}{W} \rightarrow \dot{\underset{\sim}{Q}}\,\underset{\sim}{Q}^{T} + \underset{\sim}{Q}\,\underset{\sim}{W}\,\underset{\sim}{Q}^{T} \tag{a.5}$$

The latter transformation expresses the obvious interpretation of adding the spin, $\dot{\underset{\sim}{Q}}\,\underset{\sim}{Q}^{T}$, associated with the rotation $\underset{\sim}{Q}(t)$ to the original

spin $\underset{\sim}{W}$ transformed by the superposed rotation at that time, $\underset{\sim}{Q}(t)$. A transformation of this form clearly applies to the spin of any direction embedded in the material such as a locus of material points. The appropriate spin must of course be substituted for $\underset{\sim}{W}$.

The Jaumann derivative of, for example, the shift tensor or back stress $\underset{\sim}{\alpha}$, based on any of these spins, which we will term $\underset{\sim}{\Omega}$ then takes the form

$$\dot{\underset{\sim}{\alpha}} - \underset{\sim}{\Omega}\,\underset{\sim}{\alpha} + \underset{\sim}{\alpha}\,\underset{\sim}{\Omega} \tag{a.6}$$

Under superposed rotation $\underset{\sim}{Q}(t)$ the stress type tensor $\underset{\sim}{\alpha}$ transforms as

$$\underset{\sim}{\alpha} \rightarrow \underset{\sim}{Q}\,\underset{\sim}{\alpha}\,\underset{\sim}{Q}^{T} \tag{a.7}$$

Transformation of the type (a.5) for $\underset{\sim}{\Omega}$ combined with (a.7) for $\underset{\sim}{\alpha}$ gives

$$\begin{aligned} \dot{\alpha} - \Omega\alpha + \alpha\Omega \rightarrow\ & \dot{Q}\alpha Q^{T} + Q\dot{\alpha}Q^{T} + Q\alpha\dot{Q}^{T} \\ & - (\dot{Q}Q^{T} + Q\Omega Q^{T})\,Q\alpha Q^{T} \\ & + Q\alpha Q^{T}\,(\dot{Q}Q^{T} + Q\Omega Q^{T}) \end{aligned} \tag{a.8}$$

Since $\dot{\underset{\sim}{Q}}\,\underset{\sim}{Q}^{T}$ is skew-symmetric

$$\underset{\sim}{Q}\,\underset{\sim}{\alpha}\,\underset{\sim}{Q}^{T}\,\dot{\underset{\sim}{Q}}\,\underset{\sim}{Q}^{T} = -\,\underset{\sim}{Q}\,\underset{\sim}{\alpha}\,\underset{\sim}{Q}^{T}\,\underset{\sim}{Q}\,\dot{\underset{\sim}{Q}}^{T} \tag{a.9}$$

the right hand side of (a.8) becomes

$$\underset{\sim}{Q}(\dot{\underset{\sim}{\alpha}} - \underset{\sim}{\Omega}\underset{\sim}{\alpha} + \underset{\sim}{\alpha}\underset{\sim}{\Omega})\underset{\sim}{Q}^{T} \tag{a.10}$$

Thus the Jaumann derivative is objective for the various spins used: $\underset{\sim}{W}$, $\underset{\sim}{W}^{*}$ or $\underset{\sim}{W}^{\alpha}$. This analysis is given for illustration. The properties of $\underset{\sim}{\alpha}$ in fact follow from the evolution equation (4.1) and the flow law (5.3).

It is perhaps worth observing that simple shear involves no volume change so that Cauchy stress and Kirchhoff stress are identical and the consideration

concerning the distinction between the use of these in finite-deformation plasticity theory does not arise. The constitutive equation for more general deformation briefly referred to could be taken to be in the context of rigid-plastic theory which is incompressible and exhibits the same simplification. The more general case will be addressed in a later paper.

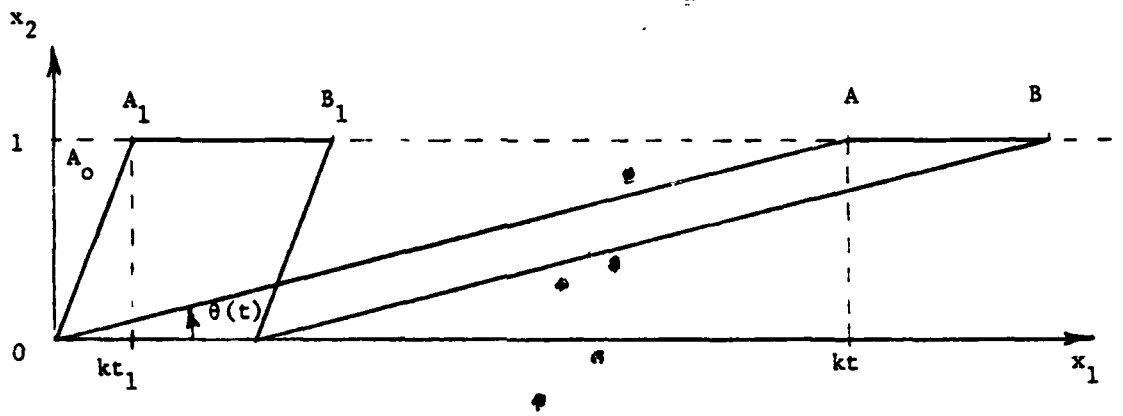

Fig. 1. Simple shear in the x_1 direction.

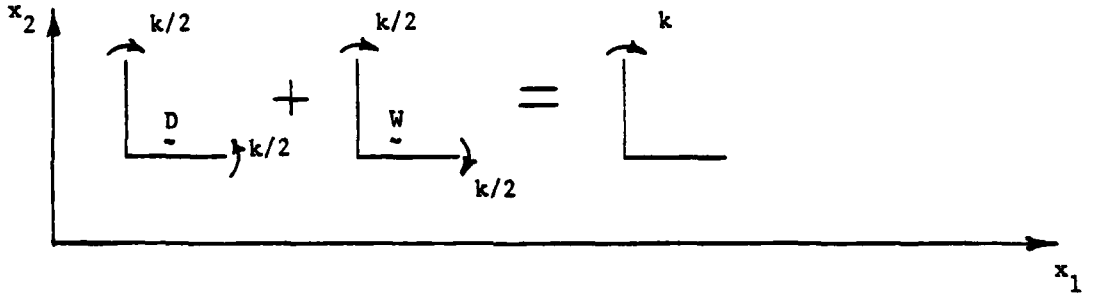

Fig. 2. Deformation rate and spin components of the velocity field.

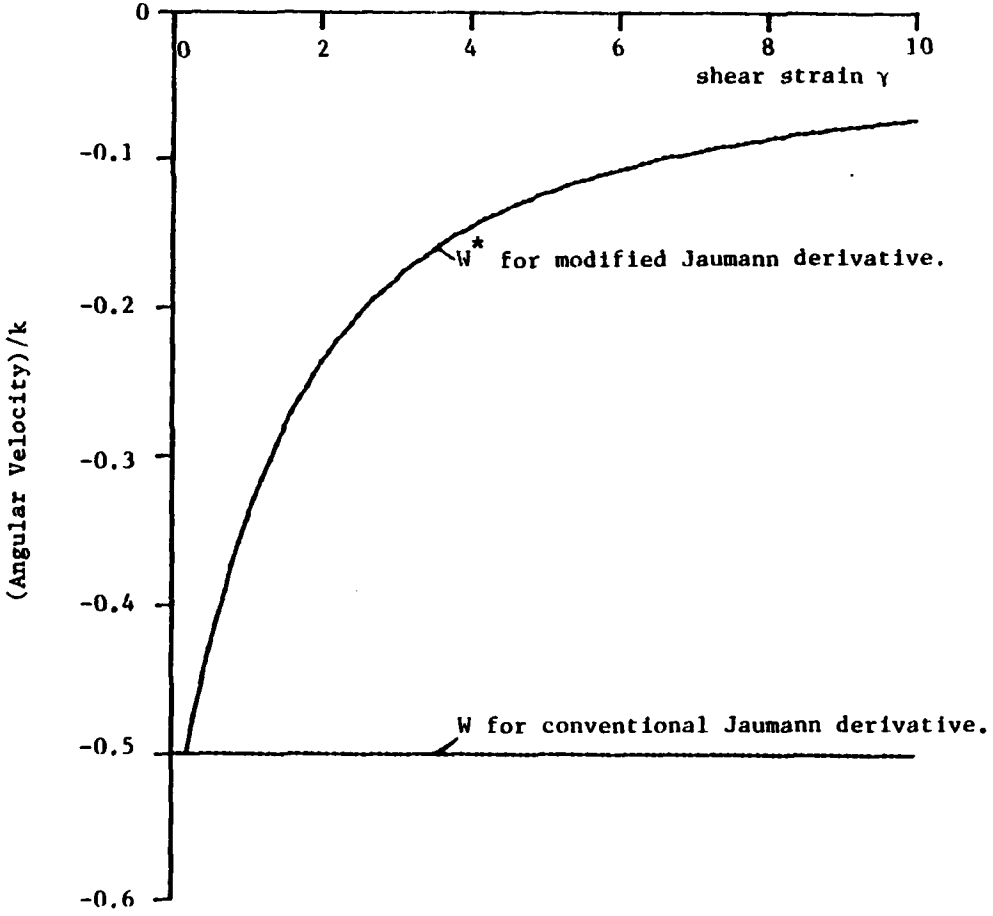

Fig. 3. Spin imparted to back-stress tensor $\underset{\sim}{\alpha}$ by material motion versus shear strain γ .

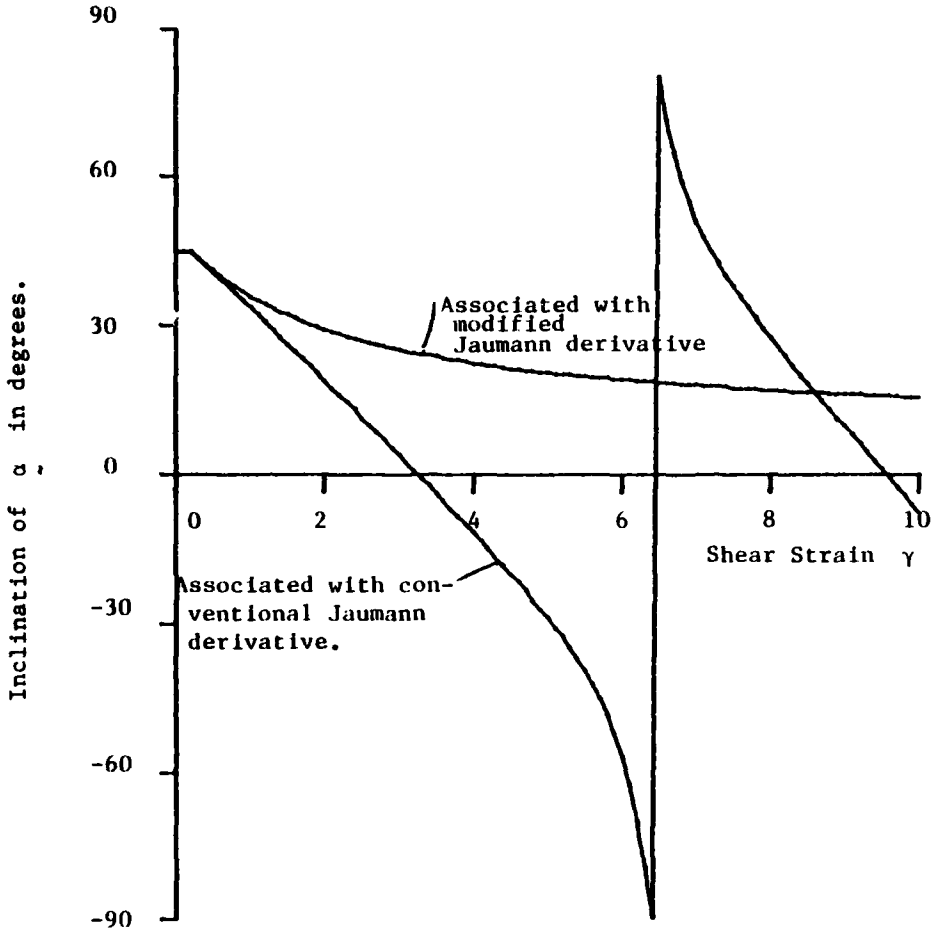

Fig. 4. Rotation of back-stress tensor $\underset{\sim}{\alpha}$ with increasing strain γ .

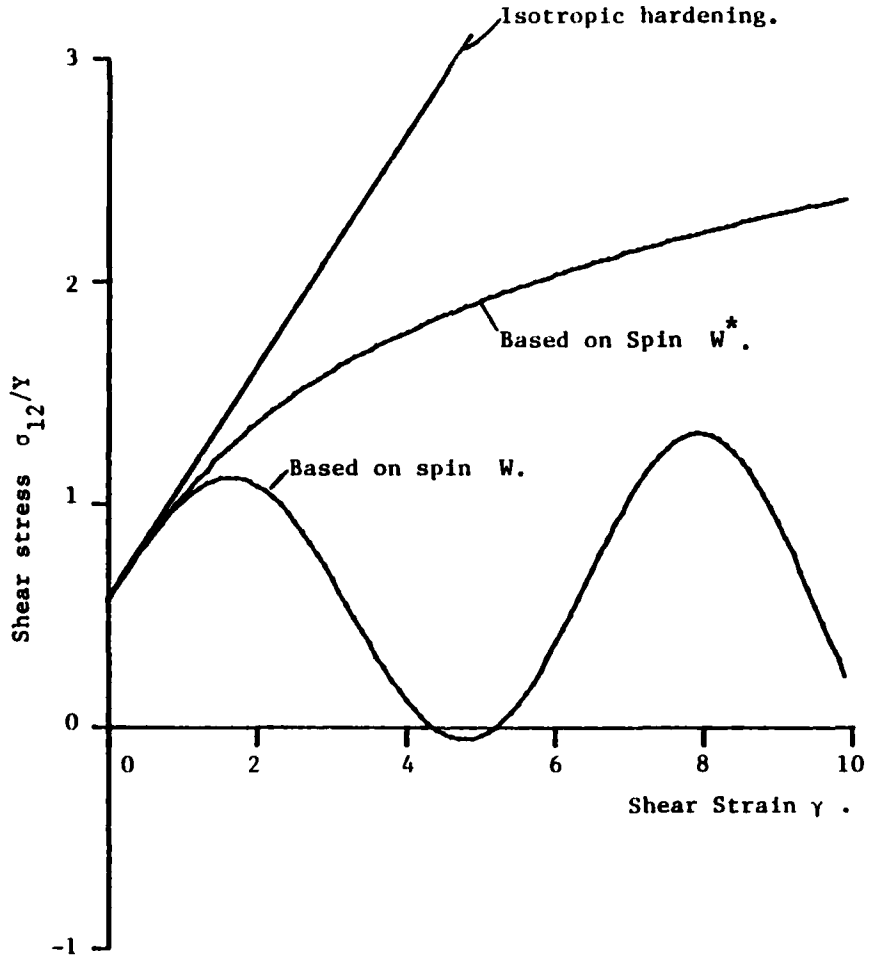

Fig. 5. Non-dimensional shear stress versus shear strain from rigid-plastic model.

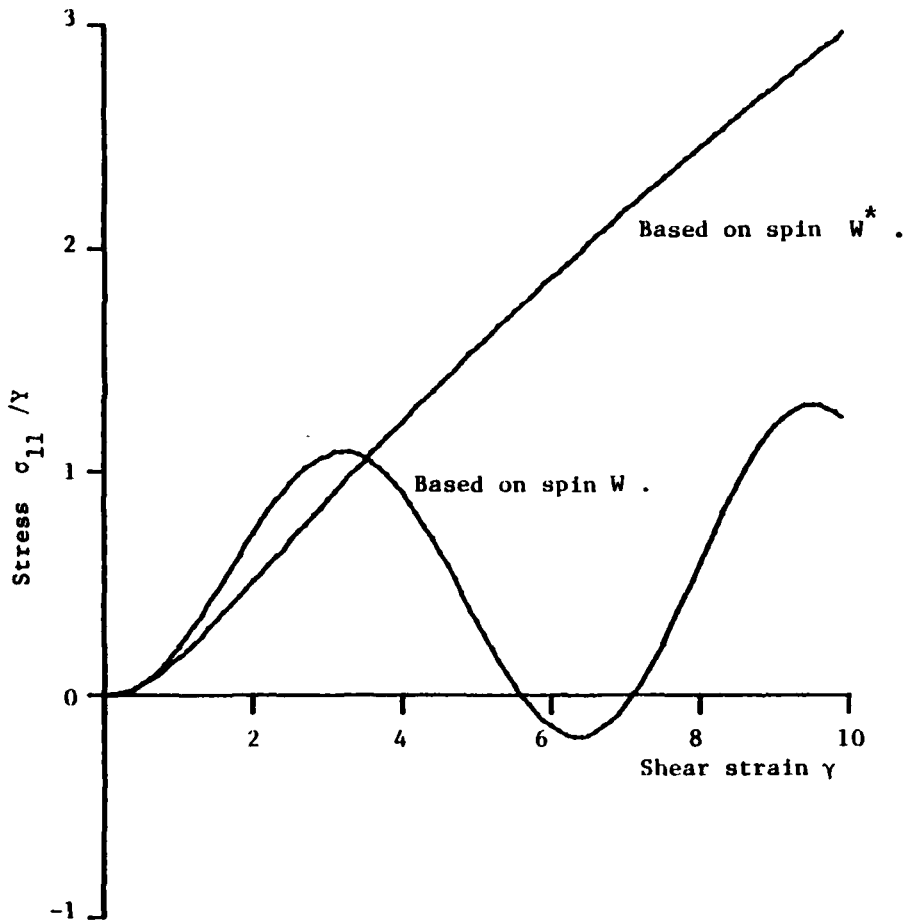

Fig. 6. Non-dimensional longitudinal stress σ_{11} versus shear strain γ for rigid-plastic model.

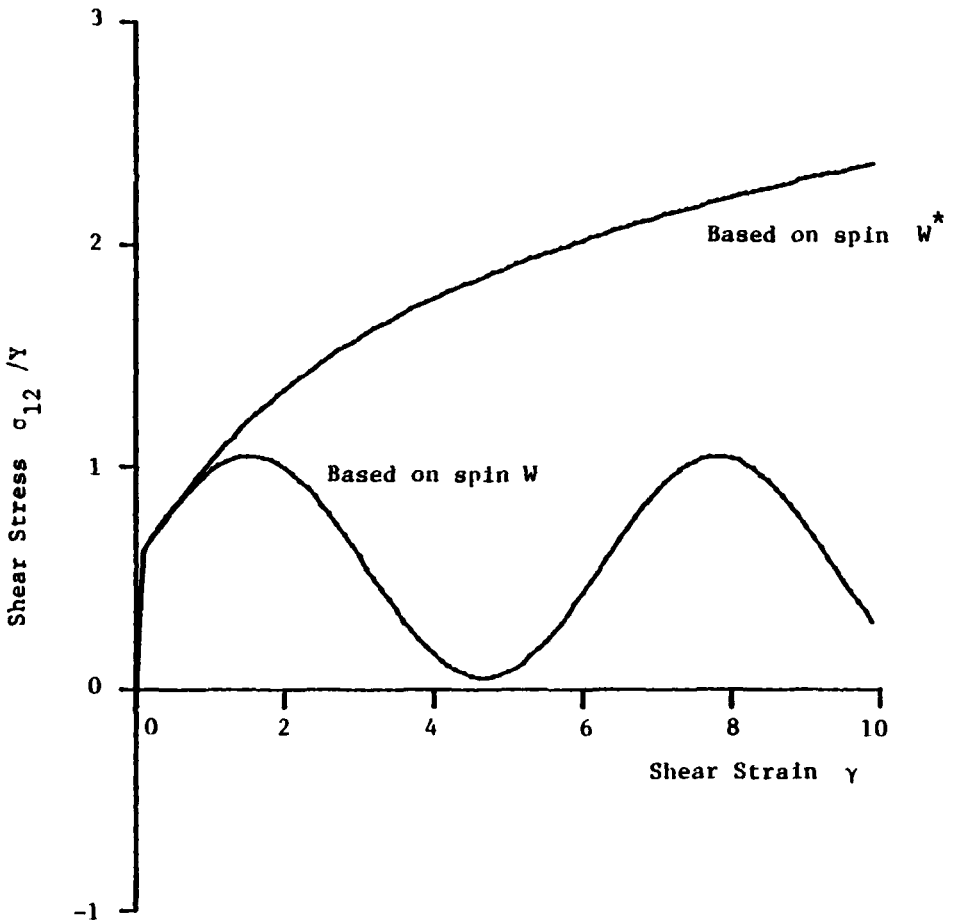

Fig. 7. Non-dimensional shear stress versus shear strain from elastic-plastic model.

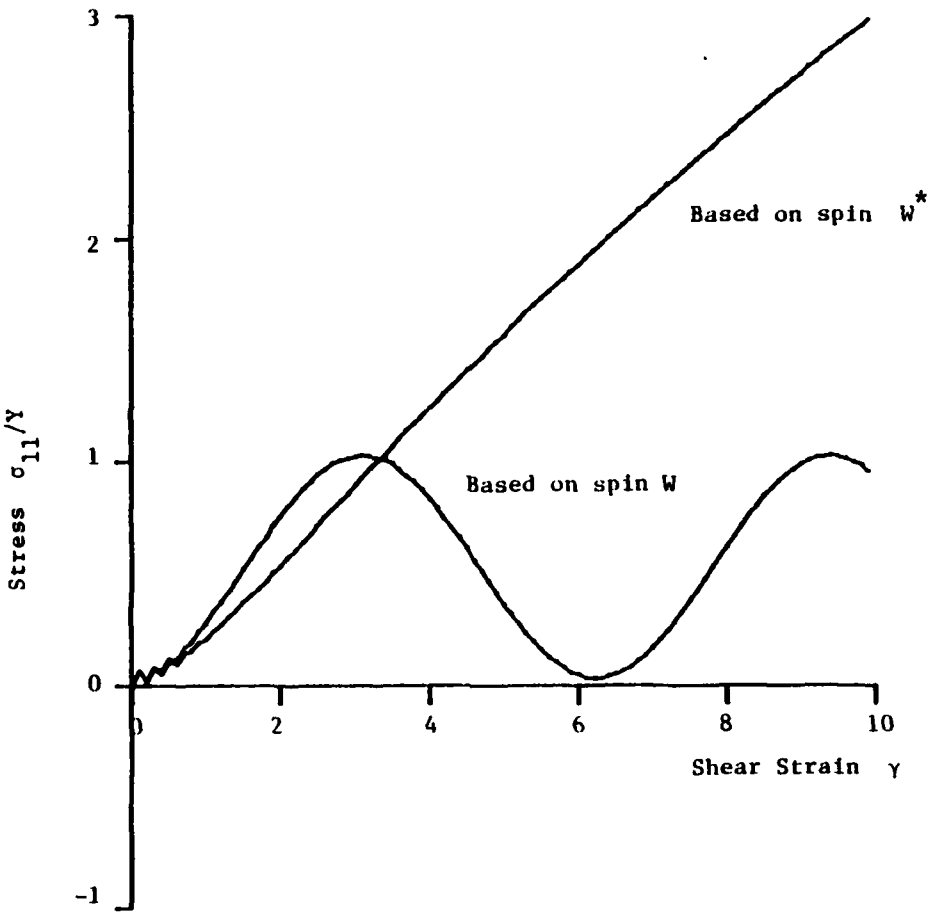

Fig. 8 Non-dimensional longitudinal stress σ_{11} versus shear strain from the elastic-plastic model.

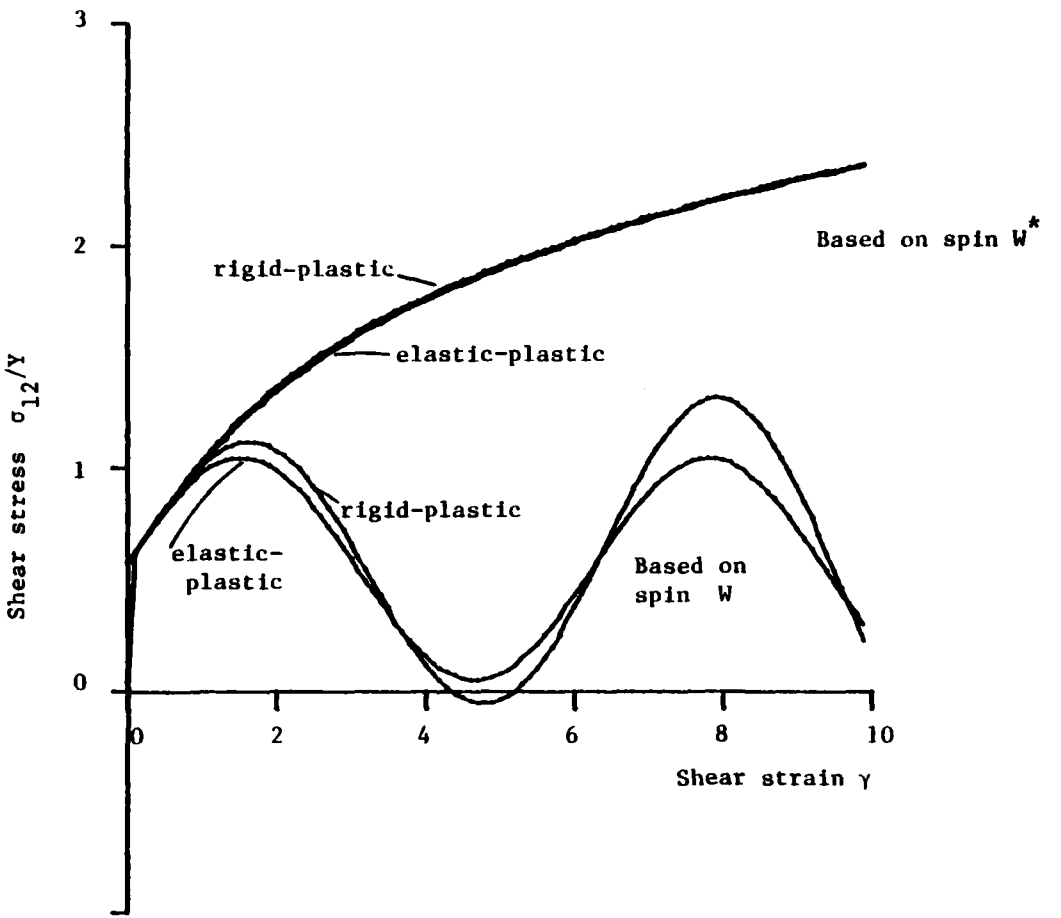

Fig. 9. Non-dimensional shear stress versus shear strain.

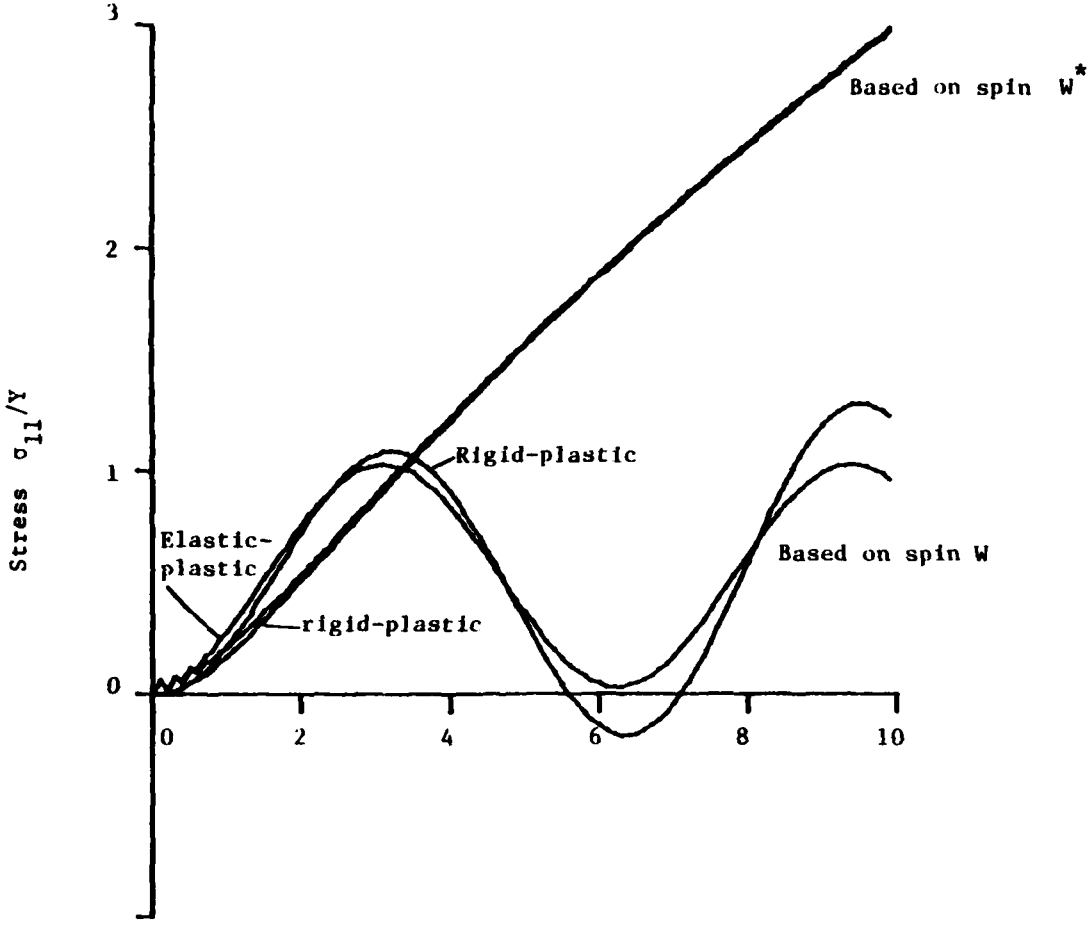

Fig. 10. Non-dimensional longitudinal stress σ_{11} versus shear strain γ .

SECURITY CLASSIFICATION OF THIS PAGE (When Data Entered)

REPORT DOCUMENTATION PAGE		READ INSTRUCTIONS BEFORE COMPLETING FORM
1. REPORT NUMBER	2. GOVT ACCESSION NO. AD-A113525	3. RECIPIENT'S CATALOG NUMBER
4. TITLE (and Subtitle) Stress Analysis for Kinematic Hardening in Finite-Deformation Plasticity		5. TYPE OF REPORT & PERIOD COVERED Final Report 7/1 - 12/1/81
		6. PERFORMING ORG. REPORT NUMBER SUDAM 81-11
7. AUTHOR(s) E. H. Lee, R. L. Mallett and T. B. Wertheimer		8. CONTRACT OR GRANT NUMBER(s) N00014-81-K-0660
9. PERFORMING ORGANIZATION NAME AND ADDRESS Division of Applied Mechanics Stanford University Stanford, Ca. 94305		10. PROGRAM ELEMENT, PROJECT, TASK AREA & WORK UNIT NUMBERS NR 064-664/4-23-81 (474)
11. CONTROLLING OFFICE NAME AND ADDRESS Office of Naval Research, 800 N. Quincy Street Arlington, Virginia 22217		12. REPORT DATE December 1981
		13. NUMBER OF PAGES 31
14. MONITORING AGENCY NAME & ADDRESS(if different from Controlling Office)		15. SECURITY CLASS. (of this report) unclassified
		15a. DECLASSIFICATION/DOWNGRADING SCHEDULE

16. DISTRIBUTION STATEMENT (of this Report)

approved for public release; distribution unlimited

17. DISTRIBUTION STATEMENT (of the abstract entered in Block 20, if different from Report)

18. SUPPLEMENTARY NOTES

19. KEY WORDS (Continue on reverse side if necessary and identify by block number)

Plasticity, finite deformation, anisotropic hardening, kinematic hardening, stress analysis, metal forming, constitutive relations.

20. ABSTRACT (Continue on reverse side if necessary and identify by block number)

Kinematic hardening represents the anisotropic component of strain hardening by a shift, $\underline{\alpha}$, of the center of the yield surface in stress space. The currently adopted approach in stress analysis at finite deformation accounts for the effect of rotation by using Jaumann derivatives of $\underline{\alpha}$ and the stress. This analysis generates the unexpected result that oscillatory shear stress is predicted for monotonically increasing simple shear strain.

continued....

DD FORM 1 JAN 73 1473 EDITION OF 1 NOV 65 IS OBSOLETE S/N 0102-LF-014-6601

SECURITY CLASSIFICATION OF THIS PAGE (When Data Entered)

Simple shear strain growing at constant rate $\dot{\gamma} = k$ yields a spin in the plane of shearing having the constant magnitude $k/2$. The effect of this on the evolution equation for the shift tensor $\underset{\sim}{\alpha}$ causes the latter to rotate continuously. In contrast, the kinematics of simple shear prescribe that no material directions rotate by more than π radians. These two features seem inconsistant since the shift tensor has its origin embedded in the material, for example as rows of dislocations piled up against grain boundaries.

By defining a modified Jaumann derivative based on the angular velocity of directions embedded in the body which characterize the effective resultant orientation of the micro-mechanisms responsible for the anisotropic hardening, a method of stress analysis is implemented which eliminates the inconsistency and yields a monotonically increasing shear stress.

Part 1 - Government
Administrative and Liaison Activities

Office of Naval Research
Department of the Navy
Arlington, Virginia 22217
Attn: Code 474 (2)
Code 471
Code 200

Director
Office of Naval Research
Branch Office
666 Summer Street
Boston, Massachusetts 02210

Director
Office of Naval Research
Branch Office
536 South Clark Street
Chicago, Illinois 60605

Director
Office of Naval Research
New York Area Office
715 Broadway - 5th Floor
New York, New York 10003

Director
Office of Naval Research
Branch Office
1030 East Green Street
Pasadena, California 91106

Naval Research Laboratory (6)
Code 2627
Washington, D.C. 20375

Defense Documentation Center (12)
Cameron Station
Alexandria, Virginia 22314

NAVY

Undersea Explosion Research Division
Naval Ship Research and Development
Center
Norfolk Naval Shipyard
Portsmouth, Virginia 23709
Attn: Dr. E. Palmer, Code 177

NAVY (Con't.)

Naval Research Laboratory
Washington, D.C. 20375
Attn: Code 6400
6410
6420
6440
6300
6390
6380

David W. Taylor Naval Ship Research
and Development Center
Annapolis, Maryland 21402
Attn: Code 2740
20
281

Naval Weapons Center
China Lake, California 93555
Attn: Code 4062
4520

Commanding Officer
Naval Civil Engineering Laboratory
Code L31
Port Hueneme, California 93041

Naval Surface Weapons Center
White Oak
Silver Spring, Maryland 20910
Attn: Code D-10
G-402
D-02

Technical Director
Naval Ocean Systems Center
San Diego, California 92152

Supervisor of Shipbuilding
U.S. Navy
Newport News, Virginia 23607

Navy Underwater Sound
Reference Division
Naval Research Laboratory
P.O. Box 8337
Orlando, Florida 32806

474:HP:716:Lab
78n674-619

NAVY (Con't.)

Chief of Naval Operations
Department of the Navy
Washington, D.C. 20350
Attn: Code OP-098

Strategic Systems Project Office
Department of the Navy
Washington, D.C. 20376
Attn: NSP-200

Naval Air Systems Command
Department of the Navy
Washington, D.C. 20361
Attn: Code 5302 (Aerospace and Structures)
604 (Technical Library)
2209 (Structures)

Naval Air Development Center
Warminster, Pennsylvania 18974
Attn: Aerospace Mechanics
Code 606

U.S. Naval Academy
Engineering Department
Annapolis, Maryland 21402

Naval Facilities Engineering Command
200 Stovall Street
Alexandria, Virginia 22332
Attn: Code 03 (Research and Development)
040
045
14114 (Technical Library)

Naval Sea Systems Command
Department of the Navy
Washington, D.C. 20362
Attn: Code 03H
312
322
323
03R
332

474:HP:716:Lab
78n674-619

NAVY (Con't.)

Commander and Director
David W. Taylor Naval Ship
Research and Development Center
Bethesda, Maryland 20084
Attn: Code 042
17
172
173
176
1800
1844
012.2
1808
1807
1843
1240
1942

Naval Underwater Systems Center
Newport, Rhode Island 02840
Attn: Dr. R. Trainor

Naval Surface Weapons Center
Dahlgren Laboratory
Dahlgren, Virginia 22448
Attn: Code G04
G20

Technical Director
Mare Island Naval Shipyard
Vallejo, California 94592

U.S. Naval Postgraduate School
Library
Code 0384
Monterey, California 93940

Webb Institute of Naval Architecture
Attn: Librarian
Crescent Beach Road, Glen Cove
Long Island, New York 11542

ARMY

Commanding Officer (2)
U.S. Army Research Office
P.O. Box 12211
Research Triangle Park, NC 27709
Attn: Mr. J. J. Murray, CRD-AA-IP

474:HP:716:Lab
78n674-619

ARMY (Con't.)

Watervliet Arsenal
MAGGS Research Center
Watervliet, New York 12189
Attn: Director of Research

U.S. Army Materials and Mechanics
Research Center
Watertown, Massachusetts 02172
Attn: Dr. E. Chen, DRXMR-T

U.S. Army Missile Research and
Development Center
Redstone Scientific Information
Center
Chief, Document Section
Redstone Arsenal, Alabama 35809

Army Research and Development
Center
Fort Belvoir, Virginia 22060

NASA

National Aeronautics and Space
Administration
Structures Research Division
Langley Research Center
Langley Station
Hampton, Virginia 23365

National Aeronautics and Space
Administration
Associate Administrator for Advanced
Research and Technology
Washington, D.C. 20546

AIR FORCE

Wright-Patterson Air Force Base
Dayton, Ohio 45433
Attn: AFFDL (FD)
(FDD)
(FBE)
(FBS)
AFML (MBM)

474:HP:716:Lab
78n674-619

AIR FORCE (Con't.)

Chief Applied Mechanics Group
U.S. Air Force Institute of Technology
Wright-Patterson Air Force Base
Dayton, Ohio 45433

Chief, Civil Engineering Branch
WLRC, Research Division
Air Force Weapons Laboratory
Kirtland Air Force Base
Albuquerque, New Mexico 87117

Air Force Office of Scientific Research
Bolling Air Force Base
Washington, D.C. 20332
Attn: Mechanics Division

Department of the Air Force
Air University Library
Maxwell Air Force Base
Montgomery, Alabama 36112

Other Government Activities

Commandant
Chief, Testing and Development Division
U.S. Coast Guard
1300 E Street, NW.
Washington, D.C. 20226

Technical Director
Marine Corps Development
and Education Command
Quantico, Virginia 22134

Director Defense Research
and Engineering
Technical Library
Room 3C128
The Pentagon
Washington, D.C. 20301

474:HP:716:Lab
78n674-619

Other Government Activities (Con't)

Dr. H. Cohn
National Science Foundation
Environmental Research Division
Washington, D.C. 20550

Library of Congress
Science and Technology Division
Washington, D.C. 20540

Director
Defense Nuclear Agency
Washington, D.C. 20305
Attn: SPSS

Mr. Jerome Persh
Staff Specialist for Materials
and Structures
OASD(I&L), The Pentagon
Room 3D1089
Washington, D.C. 20301

Chief, Airframe and Equipment Branch
FS-120
Office of Flight Standards
Federal Aviation Agency
Washington, D.C. 20553

National Academy of Sciences
National Research Council
Ship Hull Research Committee
2101 Constitution Avenue
Washington, D.C. 20418
Attn: Mr. A. R. Lytle

National Science Foundation
Engineering Mechanics Section
Division of Engineering
Washington, D.C. 20550

Picatinny Arsenal
Plastics Technical Evaluation Center
Attn: Technical Information Section
Dover, New Jersey 07801

Maritime Administration
Office of Maritime Technology
14th and Constitution Avenue, NW.
Washington, D.C. 20230

474:HP:716:Lab
78n674-619

PART 2 - Contractors and Other Technical Collaborators

Universities

Dr. J. Tinsley Oden
University of Texas at Austin
345 Engineering Science Building
Austin, Texas 78712

Professor Julius Miklowitz
California Institute of Technology
Division of Engineering
and Applied Sciences
Pasadena, California 91109

Dr. Harold Liebowitz, Dean
School of Engineering and
Applied Science
George Washington University
Washington, D.C. 20052

Professor Eli Sternberg
California Institute of Technology
Division of Engineering and
Applied Sciences
Pasadena, California 91109

Professor Paul M. Naghdi
University of California
Department of Mechanical Engineering
Berkeley, California 94720

Professor A. J. Durelli
Oakland University
School of Engineering
Rochester, Missouri 48063

Professor P. L. DiMaggio
Columbia University
Department of Civil Engineering
New York, New York 10027

Professor Norman Jones
The University of Liverpool
Department of Mechanical Engineering
P. O. Box 147
Brownlow Hill
Liverpool L69 3BX
England

Professor G. J. Simitses
Pennsylvania State University
Applied Research Laboratory
Department of Physics
State College, Pennsylvania 16801

Universities (Con't.)

Professor J. Klosner
Polytechnic Institute of New York
Department of Mechanical and
Aerospace Engineering
333 Jay Street
Brooklyn, New York 11201

Professor S. A. Schaaf
Texas A&M University
Department of Civil Engineering
College Station, Texas 77843

Professor Walter D. Pilkey
University of Virginia
Research Laboratories for the
Engineering Sciences and
Applied Sciences
Charlottesville, Virginia 22901

Professor E. D. Wilmert
Clarkson College of Technology
Department of Mechanical Engineering
Potsdam, New York 13676

Dr. Walter E. Haisler
Texas A&M University
Aerospace Engineering Department
College Station, Texas 77843

Dr. Hussein A. Kamel
University of Arizona
Department of Aerospace and
Mechanical Engineering
Tucson, Arizona 85721

Dr. S. J. Fenves
Carnegie-Mellon University
Department of Civil Engineering
Schenley Park
Pittsburgh, Pennsylvania 15213

Dr. Ronald L. Huston
Department of Engineering Analysis
University of Cincinnati
Cincinnati, Ohio 45221

474:HP:716:Lab
78m474-619

Universities (Con't)

Professor C. C. H. Lin
Lehigh University
Institute of Fracture and
Solid Mechanics
Bethlehem, Pennsylvania 18015

Professor Albert S. Kobayashi
University of Washington
Department of Mechanical Engineering
Seattle, Washington 98105

Professor Daniel Frederick
Virginia Polytechnic Institute and
State University
Department of Engineering Mechanics
Blacksburg, Virginia 24061

Professor A. C. Eringen
Princeton University
Department of Aerospace and
Mechanical Sciences
Princeton, New Jersey 08540

Professor E. H. Lee
Stanford University
Division of Engineering Mechanics
Stanford, California 94305

Professor Albert I. King
Wayne State University
Biomechanics Research Center
Detroit, Michigan 48202

Dr. V. R. Hodgson
Wayne State University
School of Medicine
Detroit, Michigan 48202

Dean B. A. Boley
Northwestern University
Department of Civil Engineering
Evanston, Illinois 60201

474:HP:716:Lab
78m474-619

Universities (Con't)

Professor P. G. Hodge, Jr.
University of Minnesota
Department of Aerospace Engineering
and Mechanics
Minneapolis, Minnesota 55455

Dr. D. C. Drucker
University of Illinois
Dean of Engineering
Urbana, Illinois 61801

Professor E. H. Dowmark
University of Illinois
Department of Civil Engineering
Urbana, Illinois 61801

Professor E. Reissner
University of California, San Diego
Department of Applied Mechanics
La Jolla, California 92037

Professor William A. Nash
University of Massachusetts
Department of Mechanics and
Aerospace Engineering
Amherst, Massachusetts 01002

Professor G. Herrmann
Stanford University
Department of Applied Mechanics
Stanford, California 94305

Professor J. N. Ashenhurst
Northwestern University
Department of Civil Engineering
Evanston, Illinois 60201

Professor S. B. Berg
University of California
Department of Mechanics
Los Angeles, California 90024

Professor Bart Paul
University of Pennsylvania
Towne School of Civil and
Mechanical Engineering
Philadelphia, Pennsylvania 19104

474:HP:716:Lab
78m474-619

Universities (Con't)

Professor H. H. Lin
Syracuse University
Department of Chemical Engineering
and Metallurgy
Syracuse, New York 13210

Professor S. Bodner
Technion R&D Foundation
Haifa, Israel

Professor Werner Goldsmith
University of California
Department of Mechanical Engineering
Berkeley, California 94720

Professor G. S. Shvin
Lehigh University
Center for the Application
of Mathematics
Bethlehem, Pennsylvania 18015

Professor F. A. Cozzarelli
State University of New York at
Buffalo
Division of Interdisciplinary Studies
Karr Parker Engineering Building
Chemistry Road
Buffalo, New York 14214

Professor Joseph L. Rose
Drexel University
Department of Mechanical Engineering
and Mechanics
Philadelphia, Pennsylvania 19104

Professor S. E. Donaldson
University of Maryland
Aerospace Engineering Department
College Park, Maryland 20742

Professor Joseph A. Clark
Catholic University of America
Department of Mechanical Engineering
Washington, D.C. 20064

474:HP:716:Lab
78m474-619

Universities (Con't)

Dr. Samuel S. Batsanf
University of California
School of Engineering
and Applied Science
Los Angeles, California 90024

Professor Isaac Fried
Boston University
Department of Mathematics
Boston, Massachusetts 02215

Professor E. Krempl
Rensselaer Polytechnic Institute
Division of Engineering
Engineering Mechanics
Troy, New York 12181

Dr. Jack R. Vinson
University of Delaware
Department of Mechanical and Aerospace
Engineering and the Center for
Composite Materials
Newark, Delaware 19711

Dr. J. Duffy
Brown University
Division of Engineering
Providence, Rhode Island 02912

Dr. J. L. Swedlow
Carnegie-Mellon University
Department of Mechanical Engineering
Pittsburgh, Pennsylvania 15213

Dr. V. K. Varadan
Ohio State University Research Foundation
Department of Engineering Mechanics
Columbus, Ohio 43210

Dr. E. Krempl
University of Pennsylvania
Department of Metallurgy and
Materials Science
College of Engineering and
Applied Science
Philadelphia, Pennsylvania 19104

474:HP:716:Lab
78m474-619

Universities (Con't)

Dr. Joshua C. S. Yang
University of Maryland
Department of Mechanical Engineering
College Park, Maryland 20742

Professor T. Y. Chang
University of Akron
Department of Civil Engineering
Akron, Ohio 44325

Professor Charles W. Bert
University of Oklahoma
School of Aerospace, Mechanical,
and Nuclear Engineering
Norman, Oklahoma 73019

Professor Satya N. Atluri
Georgia Institute of Technology
School of Engineering and
Mechanics
Atlanta, Georgia 30332

Professor Graham F. Carey
University of Texas at Austin
Department of Aerospace Engineering
and Engineering Mechanics
Austin, Texas 78712

Dr. S. S. Wang
University of Illinois
Department of Theoretical and
Applied Mechanics
Urbana, Illinois 61801

Industry and Research Institutes

Dr. Norman Hobbs
Emmet Aerilyne
Division of Lenox
Science Corporation
Burlington, Massachusetts 01803

Argonne National Laboratory
Library Services Department
9700 South Cass Avenue
Argonne, Illinois 60440

474:HP:716:Lab
78m474-619

Industry and Research Institutes (Con't)

Dr. M. C. Junger
Cambridge Acoustical Associates
54 Rindge Avenue Extension
Cambridge, Massachusetts 02140

Dr. V. Godino
General Dynamics Corporation
Electric Boat Division
Groton, Connecticut 06340

Dr. J. E. Greenspon
J. G. Engineering Research Associates
3831 Hamle Drive
Baltimore, Maryland 21215

Newport News Shipbuilding and
Dry Dock Company
Library
Newport News, Virginia 23607

Dr. V. P. Severn
McDonnell Douglas Corporation
5301 Bolsa Avenue
Huntington Beach, California 92647

Dr. S. V. Abramson
Southwest Research Institute
8500 Culebra Road
San Antonio, Texas 78284

Dr. S. C. Dehart
Southwest Research Institute
8500 Culebra Road
San Antonio, Texas 78284

Dr. N. L. Baron
Weidlinger Associates
110 East 59th Street
New York, New York 10022

Dr. T. L. Geers
Lockheed Missiles and Space Company
3251 Hanover Street
Palo Alto, California 94304

Mr. William Caywood
Applied Physics Laboratory
Johns Hopkins Road
Laurel, Maryland 20810

474:HP:716:Lab
78m474-619

Industry and Research Institutes (Con't)

Dr. Robert E. Dunham
Pacific Technology
P.O. Box 148
Del Mar, California 92014

Dr. H. P. Kamminen
Battelle Columbus Laboratories
505 King Avenue
Columbus, Ohio 43201

Dr. A. A. Membrin
Dandelion Associates, Inc.
Springtime Research Mews
13110 Frederick Road
Woodbine, Maryland 21797

Dr. James W. Jones
Dawson Services Corporation
P.O. Box 3415
Huntington Beach, California 92646

Dr. Robert E. Nickell
Applied Science and Technology
3364 North Torrey Pines Court
Suite 220
La Jolla, California 92037

Dr. Kevin Thomas
Westinghouse Electric Corp.
Advanced Reactors Division
P. O. Box 158
Madison, Pennsylvania 15663


DATE
FILMED
5-8